The pages 1–4 are title pages that will be provided by the publisher. Therefore, the table of contents starts on page V.

Beyond the odd-number limitation of time-delayed feedback control

B. Fiedler, V. Flunkert, M. Georgi, P. Hövel, and E. Schöll

March 16, 2007

Contents

List of Contributors *VII*

1 **Beyond the odd-number limitation of time-delayed feedback control** *1*
B. Fiedler, V. Flunkert, M. Georgi, P. Hövel, E. Schöll
1.1 Introduction *1*
1.2 Mechanism of stabilization *2*
1.3 Conditions on the feedback gain *7*
1.4 Conclusion *9*
Bibliography *12*

Beyond the odd-number limitation of time-delayed feedback control. B. Fiedler, V. Flunkert, M. Georgi, P. Hövel, E. Schöll

ISBN: 3-527-XXXXX-X

List of Contributors

B. Fiedler
Institut für Mathematik I
FU Berlin
Arnimallee 2-6
14195 Berlin
Germany
e-mail:
fiedler@math.fu-berlin.de

V. Flunkert
Institut für Theoretische Physik
Technische Universität Berlin
Hardenbergstraße 36
10623 Berlin
Germany
e-mail:
flunkert@itp.physik.tu-berlin.de

M. Georgi
Institut für Mathematik I
FU Berlin
Arnimallee 2-6
14195 Berlin
Germany
e-mail:
georgi@mi.fu-berlin.de

P. Hövel
Institut für Theoretische Physik
Technische Universität Berlin
Hardenbergstraße 36
10623 Berlin
Germany
e-mail:
phoevel@physik.tu-berlin.de

E. Schöll
Institut für Theoretische Physik
Technische Universität Berlin
Hardenbergstraße 36
10623 Berlin
Germany
e-mail:
schoell@physik.tu-berlin.de

Beyond the odd-number limitation of time-delayed feedback control. B. Fiedler, V. Flunkert, M. Georgi, P. Hövel, E. Schöll

ISBN: 3-527-XXXXX-X

1
Beyond the odd-number limitation of time-delayed feedback control

B. Fiedler, V. Flunkert, M. Georgi, P. Hövel, and E. Schöll[1]

1.1
Introduction

The stabilization of unstable states is a central issue in applied nonlinear science. Starting with the work of Ott, Grebogi and Yorke [1], a variety of methods have been developed in order to stabilize unstable periodic orbits (UPOs) embedded in a chaotic attractor by employing tiny control forces [2–4]. A particularly simple and efficient scheme is time-delayed feedback as suggested by Pyragas [5], which uses the difference $z(t) - z(t-\tau)$ of a signal z at a time t and a delayed time $t-\tau$. It is an attempt to stabilize periodic orbits of (minimal) period T by a feedback control which involves a time delay $\tau = nT$, for suitable positive integer n. A linear feedback example is

$$\dot{z}(t) = f(\lambda, z(t)) + B[z(t-\tau) - z(t)] \tag{1.1}$$

where $\dot{z}(t) = f(\lambda, z(t))$ describes a d-dimensional nonlinear dynamical system with bifurcation parameter λ and an unstable orbit of (minimal) period T. B is a suitably chosen constant feedback control matrix. Typical choices are multiples of the identity or of rotations, or matrices of low rank. More general nonlinear feedbacks are conceivable, of course. The main point, however, is that the Pyragas choice $\tau_P = nT$ of the delay time eliminates the feedback term on the orbit, and thus recovers the original T-periodic solution $z(t)$. In this sense the method is noninvasive.

Although time-delayed feedback control has been widely used with great success in real world problems in physics, chemistry, biology, and medicine, e.g. [6–18], see Chapters .... of this volume, severe limitations are imposed by the common belief that certain orbits cannot be stabilized for any strength of the control force. In fact, it has been contended that periodic orbits with an odd number of real Floquet multipliers greater than unity cannot be stabilized by the Pyragas method [19–24], even if the simple scheme (1.1) is extended by multiple delays in form of an infinite series [25]. To circumvent this restriction more complicated control schemes, like an oscillating feedback [26],

1) Corresponding author.

Beyond the odd-number limitation of time-delayed feedback control. B. Fiedler, V. Flunkert, M. Georgi, P. Hövel, E. Schöll

ISBN: 3-527-XXXXX-X

half-period delays for special, symmetric orbits [27], or the introduction of an additional, unstable degree of freedom [24, 28], have been proposed. In this article, we claim, and show by example, that the general limitation for orbits with an odd number of real unstable Floquet multipliers greater than unity does not hold: stabilization may be possible for suitable choices of B [29]. Our example consists of an unstable periodic orbit generated by a subcritical Hopf bifurcation. In particular, this refutes the theorem in [20].

1.2 Mechanism of stabilization

Consider the normal form of a subcritical Hopf bifurcation, extended by a time-delayed feedback term

$$\dot{z}(t) = \left[\lambda + i + (1 + i\gamma)|z(t)|^2\right] z(t) + b[z(t-\tau) - z(t)] \tag{1.2}$$

with $z \in \mathbb{C}$ and real parameters λ and γ. Here the Hopf frequency is normalized to unity. The feedback matrix B is represented by multiplication with a complex number $b = b_R + ib_I = b_0 e^{i\beta}$ with real b_R, b_I, β, and positive b_0. Note that the nonlinearity $f(\lambda, z(t)) = \left[\lambda + i + (1 + i\gamma)|z(t)|^2\right] z(t)$ commutes with complex rotations. Therefore $\exp(i\vartheta)z(t)$ solves (1.2), for any fixed ϑ, whenever $z(t)$ does. In particular, nonresonant Hopf bifurcations from the trivial solution $z \equiv 0$ at simple imaginary eigenvalues $\eta = i\omega \neq 0$ produce rotating wave solutions $z(t) = z(0)\exp\left(i\frac{2\pi}{T}t\right)$ with period $T = 2\pi/\omega$ even in the nonlinear case and with delay terms. This follows from uniqueness of the emanating Hopf branches.

Transforming Eq. (1.2) to amplitude and phase variables r, θ using $z(t) = r(t)e^{i\theta(t)}$, we obtain at $b = 0$

$$\dot{r} = \left(\lambda + r^2\right) r \tag{1.3}$$

$$\dot{\theta} = 1 + \gamma r^2. \tag{1.4}$$

An unstable periodic orbit (UPO) with $r = \sqrt{-\lambda}$ and period $T = 2\pi/(1 - \gamma\lambda)$ exists for $\lambda < 0$. This is the orbit we will stabilize. We will call it the *Pyragas orbit*. At $\lambda = 0$ a subcritical Hopf bifurcation occurs, and the steady state $z = 0$ loses its stability. The Pyragas control method chooses delays as $\tau_P = nT$. This defines the local *Pyragas curve* in the (λ, τ)-plane for any $n \in \mathbb{N}$

$$\tau_P(\lambda) = \frac{2\pi n}{1 - \gamma\lambda} = 2\pi n(1 + \gamma\lambda + \dots) \tag{1.5}$$

which emanates from the Hopf bifurcation points $\lambda = 0,\ \tau = 2\pi n$.

Under further nondegeneracy conditions, the Hopf point $\lambda = 0$, $\tau = nT$ ($n \in \mathbb{N}_0$) continues to a Hopf bifurcation curve $\tau_H(\lambda)$ for $\lambda < 0$. We determine this *Hopf curve* next. It is characterized by purely imaginary eigenvalues $\eta = i\omega$ of the transcendental characteristic equation

$$\eta = \lambda + i + b\left(e^{-\eta\tau} - 1\right) \tag{1.6}$$

which results from the linearization at the steady state $z = 0$ of the delayed system (1.2). Separating Eq. (1.6) into real and imaginary parts

$$0 = \lambda + b_0[\cos(\beta - \omega\tau) - \cos\beta] \tag{1.7}$$

$$\omega - 1 = b_0[\sin(\beta - \omega\tau) - \sin\beta] \tag{1.8}$$

and using the trigonometric identity

$$[\cos(\beta - \omega\tau)]^2 + [\sin(\beta - \omega\tau)]^2 = 1 \tag{1.9}$$

to eliminate $\omega(\lambda)$ from Eqs. (1.7),(1.8) yields an explicit expression for the multivalued Hopf curve $\tau_H(\lambda)$ for given control amplitude b_0 and phase β:

$$\tau_H = \frac{\pm \arccos\left(\frac{b_0\cos\beta - \lambda}{b_0}\right) + \beta + 2\pi n}{1 - b_0\sin\beta \mp \sqrt{\lambda(2b_0\cos\beta - \lambda) + b_0^2\sin^2\beta}}. \tag{1.10}$$

Note that τ_H is not defined in case of $\beta = 0$ and $\lambda < 0$. Thus complex b is a necessary condition for the existence of the Hopf curve in the subcritical regime $\lambda < 0$. Figure 1.1 displays the family of Hopf curves $n = 0, 1, ...$ (solid), Eq. (1.10), and the Pyragas curve $n = 1$ (dashed), Eq. (1.5), in the (λ, τ) plane. In Fig. 1.1(b) the domains of instability of the trivial steady state $z = 0$, bounded by the Hopf curves, are marked by light grey shading. The dimensions of the unstable manifold of $z = 0$ are given in parentheses along the τ-axis in Fig. 1.1(b). By construction, the delay τ becomes a multiple of the minimal period T of the bifurcating Pyragas orbits along the Pyragas curve $\tau = \tau_p(\lambda) = nT$, and the time-delayed feedback term vanishes on these periodic orbits. The inset of Fig. 1.2 displays the Hopf and Pyragas curves for different values of the feedback b_0. These choices of b_0 are displayed as full circles in the main figure, which shows the domain of control in the plane of the complex feedback gain b. For $b_0 > b_0^{crit}$ (a) the Pyragas curve runs partly inside the Hopf curve. With decreasing magnitude of b_0 the Hopf curves pull back to the right in the (λ, τ)-plane until the Pyragas curves lies fully outside the instability regime of the trivial steady state (c). At the critical feedback value (b) Pyragas and Hopf curve are tangent at $(\lambda = 0, \tau = 2\pi)$. Standard exchange of stability results [30], which hold verbatim for delay equations, then assert that the bifurcating branch of periodic solutions locally inherits linear asymptotic (in)stability from the trivial steady state, i.e., it consists of stable periodic orbits on the Pyragas curve $\tau_P(\lambda)$ inside the shaded domains

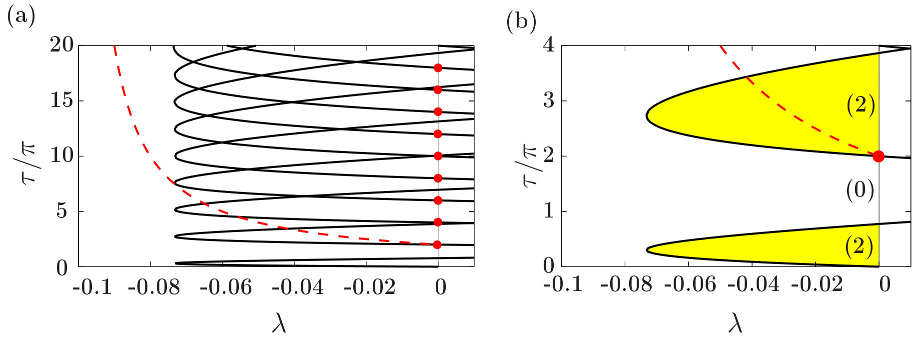

Fig. 1.1 Pyragas (dashed) and Hopf (solid) curves in the (λ, τ)-plane: (a) Hopf bifurcation curves $n = 0, ..., 10$, (b) Hopf bifurcation curves $n = 0, 1$ in an enlarged scale. Light grey shading marks the domains of unstable $z = 0$ and numbers in parentheses denote the dimension of the unstable manifold of $z = 0$ ($\gamma = -10$, $b_0 = 0.3$ and $\beta = \pi/4$).

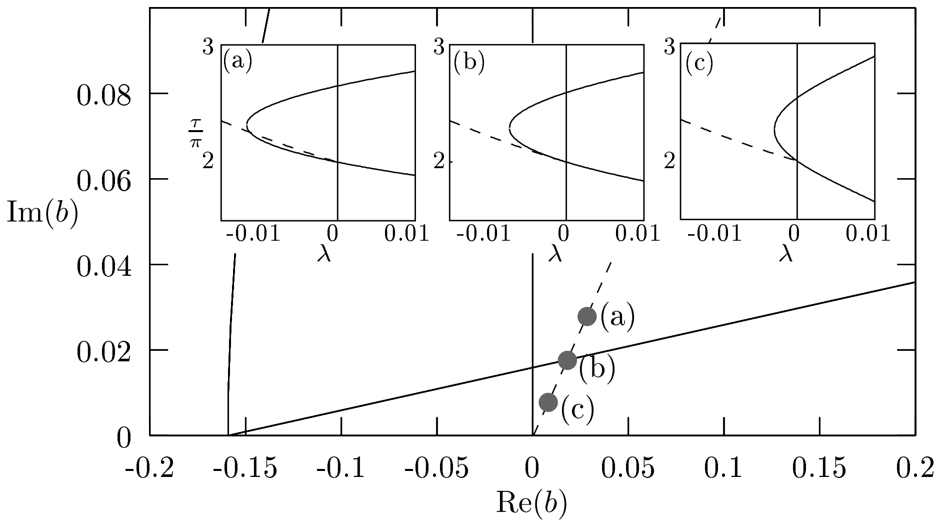

Fig. 1.2 Change of Hopf curves with varying control amplitude b_0. The main figures shows the complex plane of control gain b. The three values marked by full circles correspond to the insets (a), (b), (c), where the Hopf (solid) and Pyragas (dashed) curves are displayed for $\beta = \frac{\pi}{4}$ and three different choices of b_0: (a) $b_0 = 0.04 > b_0^{crit}$, (b)$b_0 = 0.025 \approx b_0^{crit}$ and (c) $b_0 = 0.01 < b_0^{crit}$. ($\lambda = -0.005$, $\gamma = -10$)

for small $|\lambda|$. We stress that an unstable trivial steady state is not a sufficient condition for stabilization of the Pyragas orbit. In fact, the stabilized Pyragas orbit can become unstable again if $\lambda < 0$ is further decreased, for instance in a torus bifurcation. However, there exists an interval for values of λ in our example for which the exchange of stability holds. More precisely, for small

$|\lambda|$ unstable periodic orbits possess a single Floquet multiplier $\mu = \exp(\Lambda\tau)$ with $1 < \mu < \infty$), near unity, which is simple. All other nontrivial Floquet multipliers lie strictly inside the complex unit circle. In particular, the (strong) unstable dimension of these periodic orbits is odd, here 1, and their unstable manifold is two-dimensional. This is shown in Fig. 1.3 panel (a) top, which depicts solutions Λ of the characteristic equation of the periodic solution on the Pyragas curve (see Appendix). The largest real part is positive for $b_0 = 0$.

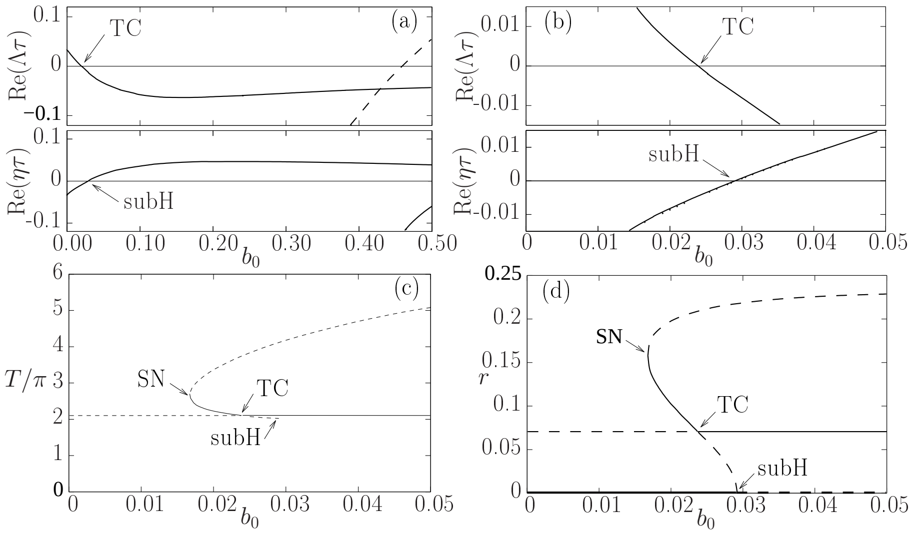

Fig. 1.3 (a) top: Real part of Floquet exponents Λ of the periodic orbit vs feedback amplitude b_0. bottom: Real part of eigenvalue η of steady state vs. feedback amplitude b_0. (b): blow-up of (a)
(c) periods and (d) radii of the periodic orbits vs. b_0. The solid and dashed curves correspond to stable and unstable periodic orbits, respectively. Parameters in all panels: $\lambda = -0.005$, $\gamma = -10$, $\tau = \frac{2\pi}{1-\gamma\lambda}$, $\beta = \pi/4$.

Thus the periodic orbit is unstable. As the amplitude of the feedback gain increases, the largest real part of the eigenvalue becomes smaller and eventually changes sign at TC. Hence the periodic orbit is stabilized. Note that an infinite number of Floquet exponents are created by the control scheme; their real parts tend to $-\infty$ in the limit $b_0 \to 0$, and some of them may cross over to positive real parts for larger b_0 (dashed line in Fig. 1.3(a)), terminating the stability of the periodic orbit.

Panel (a) bottom illustrates the stability of the steady state by displaying the largest real part of the eigenvalues η. The interesting region of the top and bottom panel where the periodic orbit becomes stable and the fixed point loses stability is magnified in panel (b).

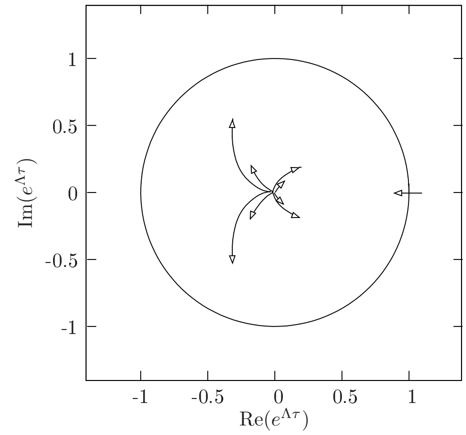

Fig. 1.4 Floquet multipliers $\mu = \exp(\Lambda\tau)$ in the complex plane with the feedback amplitude $b_0 \in [0, 0.3]$. Arrows indicate the direction of increasing b_0. Same parameters as in figure 1.3

Figure 1.4 shows the behavior of the Floquet multipliers $\mu = \exp(\Lambda\tau)$ of the Pyragas orbit in the complex plane with the increasing amplitude of the feedback gain b_0 as a parameter (marked by arrows). There is an isolated real multiplier crossing the unit circle at $\mu = 1$, in contrast to the result stated in [20]. This is caused by a transcritical bifurcation in which the Pyragas orbit collides with a delay-induced stable periodic orbit. In panel (c) and (d) of figure 1.3 the periods and radii of all circular periodic orbits ($r = const$) are plotted versus the feedback strength b_0. For small b_0 only the initial (unstable) Pyragas orbit (T and r independent of b_0) and the steady state $r = 0$ (stable) exist. With increasing b_0 a pair of unstable/stable periodic orbits is created in a saddle-node (SN) bifurcation. The stable one of the two orbits (solid) then exchanges stability with the Pyragas orbit in a transcritical bifurcation (TC), and finally ends in a subcritical Hopf bifurcation (subH), where the steady state $r = 0$ becomes unstable. The Pyragas orbit continues as a stable periodic orbit for larger b_0. Except at TC, the delay-induced orbit has a period $T \neq \tau$ (See Fig. 1.3c). Note that the respective exchanges of stability of the Pyragas orbit (TC) and the steady state (subH) occur at slightly different values of b_0. This is also corroborated by Fig. 1.3(b). The mechanism of stabilization of the Pyragas orbit by a transcritical bifurcation relies upon the possible existence of such delay-induced periodic orbits with $T \neq \tau$, which was overlooked, e.g., in [20]. Technically, the proof of the odd-number limitation theorem in [20] fails because the trivial Floquet multiplier $\mu = 1$ (Goldstone mode of periodic orbit) was neglected there; $F(1)$ in equation (14) in [20] is thus zero and not less than zero, as assumed [31]. At TC, where a second Floquet multiplier crosses the unit circle, this results in a Floquet multiplier $\mu = 1$ of algebraic multiplicity two.

1.3
Conditions on the feedback gain

Next we analyse the conditions under which stabilization of the subcritical periodic orbit is possible. From Fig. 1.1(b) it is evident that the Pyragas curve must lie inside the yellow region, i.e., the Pyragas and Hopf curves emanating from the point $(\lambda, \tau) = (0, 2\pi)$ must locally satisfy the inequality $\tau_H(\lambda) < \tau_P(\lambda)$ for $\lambda < 0$. More generally, let us investigate the eigenvalue crossings of the Hopf eigenvalues $\eta = i\omega$ along the τ-axis of Fig. 1.1. In particular we derive conditions for the unstable dimensions of the trivial steady state near the Hopf bifurcation point $\lambda = 0$ in our model equation (1.2). On the τ-axis ($\lambda = 0$), the characteristic equation (1.6) for $\eta = i\omega$ is reduced to

$$\eta = i + b\left(e^{-\eta\tau} - 1\right), \tag{1.11}$$

and we obtain two series of Hopf points given by

$$0 \leq \tau_n^A = 2\pi n \tag{1.12}$$

$$0 < \tau_n^B = \frac{2\beta + 2\pi n}{1 - 2b_0 \sin\beta} \quad (n = 0, 1, 2, \dots). \tag{1.13}$$

The corresponding Hopf frequencies are $\omega^A = 1$ and $\omega^B = 1 - 2b_0 \sin\beta$, respectively. Note that series A consists of all Pyragas points, since $\tau_n^A = nT = \frac{2\pi n}{\omega^A}$. In the series B the integers n have to be chosen such that the delay $\tau_n^B \geq 0$. The case $b_0 \sin\beta = 1/2$, only, corresponds to $\omega^B = 0$ and does not occur for finite delays τ.

We evaluate the crossing directions of the critical Hopf eigenvalues next, along the positive τ-axis and for both series. Abbreviating $\frac{\partial}{\partial\tau}\eta$ by η_τ the crossing direction is given by sign(Re η_τ). Implicit differentiation of (1.11) with respect to τ at $\eta = i\omega$ implies

$$\text{sign}(\text{Re}\,\eta_\tau) = -\text{sign}(\omega)\,\text{sign}(\sin(\omega\tau - \beta)). \tag{1.14}$$

We are interested specifically in the Pyragas-Hopf points of series A (marked by dots in Fig. 1.1) where $\tau = \tau_n^A = 2\pi n$ and $\omega = \omega^A = 1$. Indeed $\text{sign}(\text{Re}\,\eta_\tau) = \text{sign}(\sin\beta) > 0$ holds, provided we assume $0 < \beta < \pi$, i.e., $b_I > 0$ for the feedback gain. This condition alone, however, is not sufficient to guarantee stability of the steady state for $\tau < 2n\pi$. We also have to consider the crossing direction sign(Re η_τ) along series B, $\omega^B = 1 - 2b_0 \sin\beta$, $\omega^B \tau_n^B = 2\beta + 2\pi n$, for $0 < \beta < \pi$. Equation (1.14) now implies $\text{sign}(\text{Re}\,\eta_\tau) = \text{sign}((2b_0 \sin\beta - 1)\sin\beta) = \text{sign}(2b_0 \sin\beta - 1)$.

To compensate for the destabilization of $z = 0$ upon each crossing of any point $\tau_n^A = 2\pi n$, we must require stabilization (sign(Re η_τ) < 0) at each point τ_n^B of series B. If $b_0 \geq 1/2$, this requires $0 < \beta < \arcsin(1/(2b_0))$ or $\pi - \arcsin(1/(2b_0)) < \beta < \pi$. The distance between two successive points τ_n^B and τ_{n+1}^B is $2\pi/\omega^B > 2\pi$. Therefore, there is at most one τ_n^B between any two successive Hopf points of series A. Stabilization requires exactly one such τ_n^B, specifically: $\tau_{k-1}^A < \tau_{k-1}^B < \tau_k^A$ for all $k = 1, 2, \ldots$,n. This condition is satisfied if, and only if,

$$0 < \beta < \beta_n^*, \tag{1.15}$$

where $0 < \beta_n^* < \pi$ is the unique solution of the transcendental equation

$$\frac{1}{\pi}\beta_n^* + 2nb_0 \sin\beta_n^* = 1. \tag{1.16}$$

This holds because the condition $\tau_{k-1}^A < \tau_{k-1}^B < \tau_k^A$ first fails when $\tau_{k-1}^B = \tau_k^A$. Equation (1.15) represents a necessary but not yet sufficient condition that the Pyragas choice $\tau_P = nT$ for the delay time will stabilize the periodic orbit.

To evaluate the remaining condition, $\tau_H < \tau_P$ near $(\lambda, \tau) = (0, 2\pi)$, we expand the exponential in the characteristic equation (1.6) for $\omega\tau \approx 2\pi n$, and obtain the approximate Hopf curve for small $|\lambda|$:

$$\tau_H(\lambda) \approx 2\pi n - \frac{1}{b_I}(2\pi n b_R + 1)\lambda. \tag{1.17}$$

Recalling (1.5), the Pyragas stabilization condition $\tau_H(\lambda) < \tau_P(\lambda)$ is therefore satisfied for $\lambda < 0$ if, and only if,

$$\frac{1}{b_I}\left(b_R + \frac{1}{2\pi n}\right) < -\gamma. \tag{1.18}$$

Equation(1.18) defines a domain in the plane of the complex feedback gain $b = b_R + ib_I = b_0 e^{i\beta}$ bounded from below (for $\gamma < 0 < b_I$) by the straight line

$$b_I = \frac{1}{-\gamma}\left(b_R + \frac{1}{2\pi n}\right). \tag{1.19}$$

Equation (1.16) represents a curve $b_0(\beta)$, i.e.,

$$b_0 = \frac{1}{2n\sin\beta}\left(1 - \frac{\beta}{\pi}\right), \tag{1.20}$$

which forms the upper boundary of a domain given by the inequality (1.15). Thus Eqs. (1.19) and (1.20) describe the boundaries of the domain of control in the complex plane of the feedback gain b in the limit of small λ. Fig.1.5 depicts this domain of control for $n = 1$, i.e., a time delay $\tau = \frac{2\pi}{1-\gamma\lambda}$. The lower and upper solid curves correspond to Eq. (1.19) and Eq. (1.20), respectively. The grayscale displays the numerical result of the largest real part, wherever < 0, of the Floquet exponent, calculated from linearization of the amplitude and phase equations around the periodic orbit (Appendix). Outside the shaded areas the periodic orbit is not stabilized. With increasing $|\lambda|$ the domain of stabilization shrinks, as the deviations from the linear approximation (1.17) become larger. For sufficiently large $|\lambda|$ stabilization is no longer possible, in agreement with Fig.1.1(b). Note that for real values of b, i.e., $\beta = 0$, no stabilization occurs at all. Hence, stabilization fails if the feedback matrix B is a multiple of the identity matrix. Fig. 1.6 compares the control domain for the same value of $|\lambda|$ for the representation in the planes of complex feedback b (left), and amplitude b_0 and phase β (right).

1.4 Conclusion

In conclusion, we have refuted a theorem which claims that a periodic orbit with an odd number of real Floquet multipliers greater than unity can never be stabilized by time-delayed feedback control. For this purpose we have analysed the generic example of the normal form of a subcritical Hopf bifurcation, which is paradigmatic for a large class of nonlinear systems. We have worked out explicit analytical conditions for stabilization of the periodic orbit generated by a subcritical Hopf bifurcation in terms of the amplitude and the phase of the feedback control gain [32]. Our results underline the crucial role of a non-vanishing phase of the control signal for stabilization of periodic orbits violating the odd-number limitation. The feedback phase is readily accessible and can be adjusted, for instance, in laser systems, where subcritical Hopf bifurcation scenarios are abundant and Pyragas control can be realized via coupling to an external Fabry-Perot resonator [18]. The importance of the feedback phase for the stabilization of steady states in lasers [18] and neural systems [33], as well as for stabilization of periodic orbits by a time-delayed feedback control scheme using spatio-temporal filtering [34], has been noted recently. Here, we have shown that the odd-number limitation does not hold in general, which opens up fundamental questions as well as a wide range of applications. The result will not only be important for practical applications in physical sciences, technology, and life sciences, where one might often desire to stabilize periodic orbits with an odd number of positive Floquet exponents, but also for tracking of unstable orbits and bifurcation analysis using time-delayed feedback control [35].

Acknowledgements
This work was supported by Deutsche Forschungsgemeinschaft in the frame-

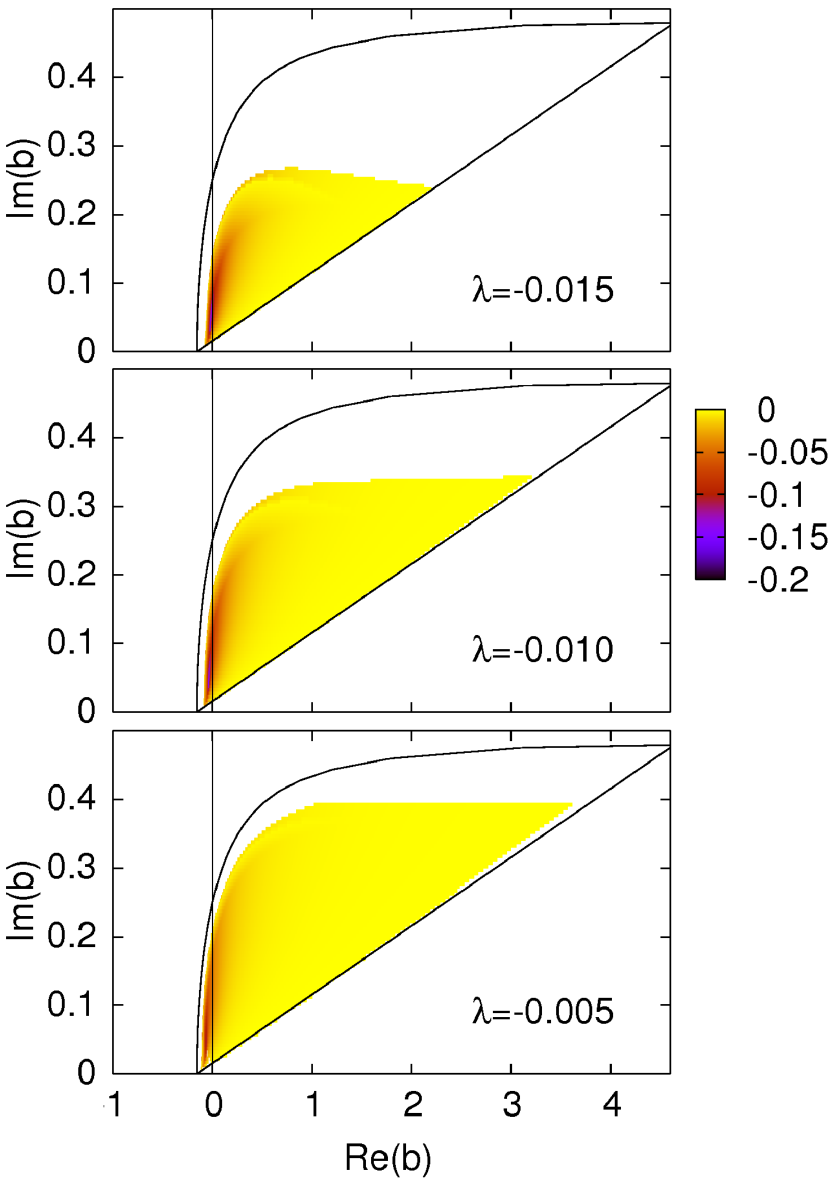

Fig. 1.5 Domain of control in the plane of the complex feedback gain $b = b_0 e^{i\beta}$ for three different values of the bifurcation parameter λ. The solid curves indicate the boundary of stability in the limit $\lambda \nearrow 0$, see (1.19), (1.20). The shading shows the magnitude of the largest (negative) real part of the Floquet exponents of the periodic orbit ($\gamma = -10$, $\tau = \frac{2\pi}{1-\gamma\lambda}$).

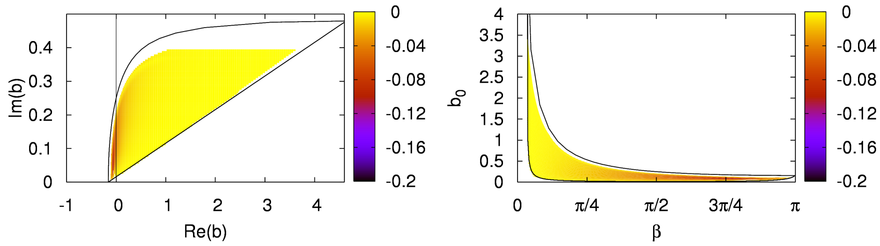

Fig. 1.6 Domain of control in the complex b-plane (left) and the β-b_0-plane (right) ($\lambda = -0.005$, $\gamma = -10$, $\tau = \frac{2\pi}{1-\gamma\lambda}$).

work of Sfb 555. We acknowledge useful discussions with A. Amann, W. Just, and A. Pikovsky.

Appendix: Calculation of Floquet exponents

The Floquet exponents of the Pyragas orbit can be calculated explicitly by rewriting Eq. (1.2) in polar coordinates $z = r\, e^{i\theta}$

$$\dot{r} \;=\; (\lambda + r^2)\, r + b_0[\cos(\beta + \theta(t-\tau) - \theta)\, r(t-\tau) - \cos(\beta)\, r] \quad (1.21)$$

$$\dot{\theta} \;=\; 1 + \gamma r^2 + b_0[\sin(\beta + \theta(t-\tau) - \theta)\, \frac{r(t-\tau)}{r} - \sin(\beta)] \quad (1.22)$$

and linearizing around the periodic orbit according to $r(t) = r_0 + \delta r(t)$ and $\theta(t) = \Omega t + \delta\theta(t)$, with $r_0 = \sqrt{-\lambda}$ and $\Omega = 1 - \gamma\lambda$ (see Eq. (1.3)). This yields

$$\begin{pmatrix} \dot{\delta r}(t) \\ \dot{\delta\theta}(t) \end{pmatrix} = \begin{bmatrix} -2\lambda - b_0 \cos\beta & b_0 r_0 \sin\beta \\ 2\gamma r_0 - b_0 \sin\beta\, r_0^{-1} & -b_0 \cos\beta \end{bmatrix} \begin{pmatrix} \delta r(t) \\ \delta\theta(t) \end{pmatrix} \quad (1.23)$$

$$+ \begin{bmatrix} b_0 \cos\beta & -b_0 r_0 \sin\beta \\ b_0 \sin\beta r_0^{-1} & b_0 \cos\beta \end{bmatrix} \begin{pmatrix} \delta r(t-\tau) \\ \delta\theta(t-\tau) \end{pmatrix}. \quad (1.24)$$

With the ansatz

$$\begin{pmatrix} \delta r(t) \\ \delta\theta(t) \end{pmatrix} = u\ \exp(\Lambda t), \quad (1.25)$$

where u is a two-dimensional vector, one obtains the autonomous linear equation

$$\begin{bmatrix} -2\lambda + b_0 \cos\beta\, (e^{-\Lambda\tau} - 1) - \Lambda & -b_0 r_0 \sin\beta\, (e^{-\Lambda\tau} - 1) \\ 2\gamma r_0 + b_0 r_0^{-1} \sin\beta\, (e^{-\Lambda\tau} - 1) & b_0 \cos\beta\, (e^{-\Lambda\tau} - 1) - \Lambda \end{bmatrix} u = 0. \quad (1.26)$$

The condition of vanishing determinant then gives the transcendental characteristic equation

$$0 = \left(-2\lambda + b_0 \cos\beta\,(e^{-\Lambda\tau} - 1) - \Lambda\right)\left(b_0 \cos\beta\,(e^{-\Lambda\tau} - 1) - \Lambda\right) \quad (1.27)$$

$$-b_0 r_0 \sin\beta\,(e^{-\Lambda\tau} - 1)\left(2\gamma r_0 + b_0 r_0^{-1} \sin\beta\,(e^{-\Lambda\tau} - 1)\right) \quad (1.28)$$

for the Floquet exponents Λ which can be solved numerically.

Bibliography

1 E. Ott, C. Grebogi, and J. A. Yorke: *Controlling chaos*, Phys. Rev. Lett. **64**, 1196 (1990).

2 H. G. Schuster (Editor): *Handbook of Chaos Control* (Wiley-VCH, Weinheim, 1st edition, 1999).

3 S. Boccaletti, C.Grebogi, Y. C. Lai, H. Mancini, and D. Maza: *The control of chaos: theory and applications*, Phys. Rep. **329**, 103 (2000).

4 D. J. Gauthier: *Resource letter: Controlling chaos*, Am. J. Phys. **71**, 750 (2003).

5 K. Pyragas: *Continuous control of chaos by self-controlling feedback*, Phys. Lett. A **170**, 421 (1992).

6 K. Pyragas and A. Tamaševičius: *Experimental control of chaos by delayed self-controlling feedback*, Phys. Lett. A **180**, 99 (1993).

7 S. Bielawski, D. Derozier, and P. Glorieux: *Controlling unstable periodic orbits by a delayed continuous feedback*, Phys. Rev. E **49**, R971 (1994).

8 T. Pierre, G. Bonhomme, and A. Atipo: *Controlling the chaotic regime of nonlinear ionization waves using time-delay autsynchronisation method*, Phys. Rev. Lett. **76**, 2290 (1996).

9 K. Hall, D. J. Christini, M. Tremblay, J. J. Collins, L. Glass, and J. Billette: *Dynamic control of cardiac alterans*, Phys. Rev. Lett. **78**, 4518 (1997).

10 D. W. Sukow, M. E. Bleich, D. J. Gauthier, and J. E. S. Socolar: *Controlling chaos in a fast diode resonator using time-delay autosynchronisation: Experimental observations and theoretical analysis*, Chaos **7**, 560 (1997).

11 O. Lüthje, S. Wolff, and G. Pfister: *Control of chaotic taylor-couette flow with time-delayed feedback*, Phys. Rev. Lett. **86**, 1745 (2001).

12 P. Parmananda, R. Madrigal, M. Rivera, L. Nyikos, I. Z. Kiss, and V. Gáspár: *Stabilization of unstable steady states and periodic orbits in an electrochemical system using delayed-feedback control*, Phys. Rev. E **59**, 5266 (1999).

13 J. M. Krodkiewski and J. S. Faragher: *Stabilization of motion of helicopter rotor blades using delayed feedback - modelling, computer simulation and experimental verification*, J. Sound Vib. **234**, 591 (2000).

14 T. Fukuyama, H. Shirahama, and Y. Kawai: *Dynamical control of the chaotic state of the current-driven ion acoustic instability in a laboratory plasma using delayed feedback*, Phys. Plasmas **9**, 4525 (2002).

15 C. von Loewenich, H. Benner, and W. Just: *Experimental relevance of global properties of time-delayed feedback control*, Phys. Rev. Lett. **93**, 174101 (2004).

16 M. G. Rosenblum and A. S. Pikovsky: Phys. Rev. Lett. **92**, 114102 (2004).

17 O. V. Popovych, C. Hauptmann, and P. A. Tass: *Effective desynchronization by nonlinear delayed feedback*, Phys. Rev. Lett. **94**, 164102 (2005).

18 S. Schikora, P. Hövel, H.-J. Wünsche, E. Schöll, and F. Henneberger: *All-optical noninvasive control of unstable steady states in a semiconductor laser*, Phys. Rev. Lett. **97**, 213902 (2006).

19 W. Just, T. Bernard, M. Ostheimer, E. Reibold, and H. Benner: *Mechanism of time-delayed feedback control*, Phys. Rev. Lett. **78**, 203 (1997).

20 H. Nakajima: *On analytical properties of delayed feedback control of chaos*, Phys. Lett. A **232**, 207 (1997).

21 H. Nakajima and Y. Ueda: *Limitation of generalized delayed feedback control*, Physica D **111**, 143 (1998).

22 I. Harrington and J. E. S. Socolar: *Limitation on stabilizing plane waves via time-delay feedback*, Phys. Rev. E **64**, 056206 (2001).

23 K. Pyragas, V. Pyragas, and H. Benner: *Delayed feedback control of dynamical systems at subcritical Hopf bifurcation*, Phys. Rev. E **70**, 056222 (2004).

24 V. Pyragas and K. Pyragas: *Delayed feedback control of the Lorentz system: An analytical treatment at a subcritical Hopf bifurcation*, Phys. Rev. E **73**, 036215 (2006).

25 J. E. S. Socolar, D. W. Sukow, and D. J. Gauthier: *Stabilizing unstable periodic orbits in fast dynamical systems*, Phys. Rev. E **50**, 3245 (1994).

26 H. G. Schuster and M. B. Stemmler: *Control of chaos by oscillating feedback*, Phys. Rev. E **56**, 6410 (1997).

27 H. Nakajima and Y. Ueda: *Half-period delayed feedback control for dynamical systems with symmetries*, Phys. Rev. E **58**, 1757 (1998).

28 K. Pyragas: *Control of chaos via an unstable delayed feedback controller*, Phys. Rev. Lett. **86**, 2265 (2001).

29 B. Fiedler, V. Flunkert, M. Georgi, P. Hövel, and E. Schöll: *Refuting the odd-number limitation of time-delayed feedback control*, Phys. Rev. Lett. **98**, 114101 (2007).

30 O. Diekmann, S. A. van Gils, S. M. V. Lunel, and H.-O. Walther: *Delay Equations* (Springer-Verlag, New York, 1995).

31 A. Amann (private communication).

32 For the complex conjugate values of b, stabilization of the periodic orbit can be shown by analogous arguments.

33 M. G. Rosenblum and A. S. Pikovsky: *Delayed feedback control of collective synchrony: An approach to suppression of pathological brain rhythms*, Phys. Rev. E **70**, 041904 (2004).

34 N. Baba, A. Amann, E. Schöll, and W. Just: *Giant improvement of time-delayed feedback control by spatio-temporal filtering*, Phys. Rev. Lett. **89**, 074101 (2002).

35 J. Sieber and B. Krauskopf: *Control based bifurcation analysis for experiments*, Nonlinear Dynamics, DOI: 10.1007/s11071-007-9217-2 (2007)